IEEE Access
Multidisciplinary | Rapid Review | Open Access Journal

SPECIAL SECTION ON OPTICAL WIRELESS TECHNOLOGIES FOR 5G COMMUNICATIONS AND BEYOND

Received July 31, 2017, accepted September 1, 2017, date of publication September 15, 2017, date of current version October 12, 2017.

Digital Object Identifier 10.1109/ACCESS.2017.2753178

Impact of Fiber Nonlinearity on 5G Backhauling via Mixed FSO/Fiber Network

AHMED E. MORRA[1,2], (Member, IEEE), KHALED AHMED[1], AND STEVE HRANILOVIC[1], (Senior Member, IEEE)

[1]Department of Electrical and Computer Engineering, McMaster University, Hamilton, ON L8S 4K1, Canada
[2]Electronics and Electrical Communications Engineering Department, Faculty of Electronic Engineering, Menoufia University, Menouf 32952, Egypt

Corresponding author: Ahmed E. Morra (morraa1@mcmaster.ca; ahmed.morra@el-eng.menofia.edu.eg)

This work was supported in part by Telus Corporation and in part by the Natural Sciences and Engineering Research Council of Canada.

ABSTRACT The inherently high bandwidth of fiber and free-space optical (FSO) links make them ideally suited to provide broadband backhaul in fifth-generation (5G) mobile networks. However, both fiber and FSO systems suffer from a variety of impairments, which must be properly modeled in order to design the network. In this paper, we present analytical results for mixed FSO/fiber amplify-and-forward backhauling systems, where the impacts of radio-frequency (RF) co-channel interference, FSO pointing errors, and both fiber and FSO modulator nonlinearity are modeled and taken into consideration. Closed-form and asymptotic expressions are derived for the outage probability, the average bit-error rate, and the cumulative distribution function (CDF) of the channel capacity for mixed FSO/fiber backhauling systems. Our results reveal an optimal average-launched power for the fiber, which balances the impact of fiber nonlinear distortion with the receiver noise. In particular, when using the optimal fiber average-launched power, our estimated user capacity CDF results show that the 50th percentile user rates using mm-wave RF access can reach over 1.5 Gb/s in ideal conditions. However, user rates are more sensitive to the FSO backhaul channel characteristics.

INDEX TERMS Amplify-and-forward, atmospheric turbulence, co-channel interference, fiber nonlinearity, free-space optics (FSO), modulator clipping, pointing errors.

I. INTRODUCTION

Fifth-generation (5G) networks have promised impressive improvements in network performance at the cost of extreme cell densification [1]–[3]. Given the ultra-dense and widespread deployment of radio units in 5G, energy and cost effective backhaul networks are essential to realize the potential of 5G systems. Though fiber backhaul is preferred, it is often not available or expensive to install. Backhaul using free-space optical (FSO) links, though sensitive to weather conditions, provides inexpensive, huge bandwidth links and serves as an efficient backhauling bridge between radio-frequency (RF) access and central fiber backhaul nodes [4], [5]. This paper considers the design of 5G networks with mixed FSO and fiber backhaul by considering the unique impairments inherent to both media. In particular, low complexity amplify-and-forward (AF) backhaul links are considered due to their low cost and energy requirements.

Free-space optics as a backhauling medium for radio systems has recently received increasing attention in the literature. Most studies consider outage performance, bit error rate (BER), and ergodic capacity results under a variety of statistical channel models for RF and FSO channels [4]–[16]. Lee *et al.* [6] presented the first analysis of outage performance of a dual-hop AF relay system consisting of RF and FSO links with Rayleigh and gamma-gamma distributed channel gains respectively. As an extension to [6], the impact of pointing errors on the BER performance and the ergodic capacity of a mixed AF RF/FSO systems was then carried out in [7]. Based on outdated channel state information (CSI), Petkovic *et al.* [8] studied dual-hop AF with relay selection RF/FSO multiple relay systems. In [9] and [10], an outage probability expression was derived for a fixed AF RF/FSO system which is corrupted by both noise and co-channel interference while assuming that the relay gain is selected based on outdated CSI. Soleimani-Nasab and Uysal present a comprehensive survey and analysis of AF RF/FSO systems which includes the impact of co-channel interference and pointing errors, where the RF and FSO links were distributed according to Nakagami-*m* and double generalized gamma distributions, respectively [5].

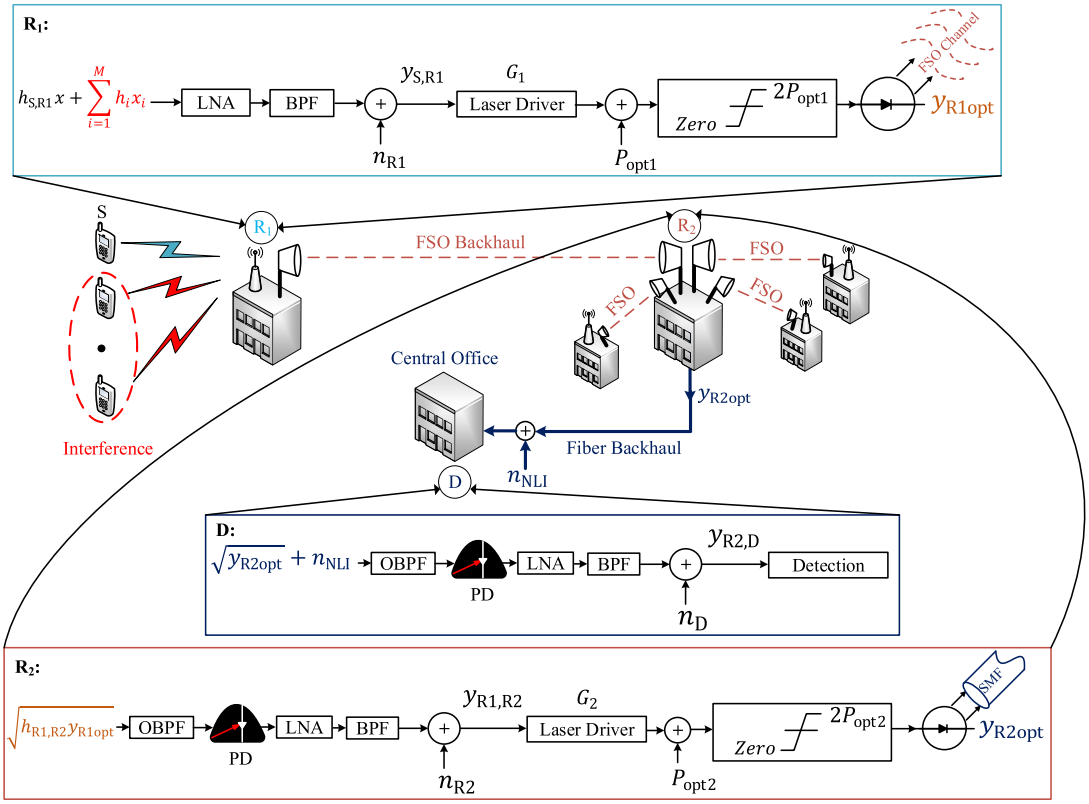

FIGURE 1. RF/FSO/Fiber hybrid architecture for 5G access and backhaul networks.

In this paper, we extend earlier work on FSO backhauling by including a fiber optical link to aggregate the backhaul from multiple FSO units in a 5G network. As shown in Fig. 1, received signals from a radio access network are AF-relayed over an FSO link and multiple such backhaul channels are AF-relayed over a fiber trunk. Like earlier work, co-channel interference, pointing errors, and scintillation of the FSO links are considered explicitly. The multipath fading in the RF links is assumed to follow a Rayleigh fading distribution and the FSO link is assumed to have a gamma-gamma atmospheric turbulence fading distribution. Additionally, the effect of the nonlinearity of the FSO and fiber relay nodes is taken into consideration here by selecting the gain to ensure negligible clipping likelihood. For AF relaying over the fiber, the impact of nonlinear propagation on the performance of the system can be significant. Here we employ the Gaussian noise (GN) model [17] to quantify the impact of fiber nonlinearities which is tractable and widely used for system design and analysis [18]–[22]. Under the assumption of AF relaying, closed-form expressions are derived for the outage probability, the average bit-error rate (BER), and the cumulative distribution function (CDF) of user capacities of the network using a mixed FSO/fiber backhaul system. In addition, asymptotic expressions at high FSO and fiber signal-to-noise ratios (SNRs) are derived to provide useful physical insights. The optimal average launched fiber power is derived, in the case of high SNR at both the FSO and fiber links, and shown to provide good performance over a variety of practical scenarios.

The balance of the paper is organized as follows. In Section II, system and the channels model are presented. Outage probability, capacity-CDF, and the average BER expressions are derived in Sections III and IV, while asymptotic results are given in Section V. Section VI provides numerical results on the performance evaluation using a mm-wave radio access network and mixed FSO/fiber backhaul. Finally, the conclusions are summarized in Section VII.

II. SYSTEM AND CHANNEL MODELS

As shown in Fig. 1, the system consists of an RF access medium corrupted by interference and a mixed FSO/fiber backhaul. Two AF relays, R_1 and R_2, forward received signals from the source node, S, to the destination node, D, using FSO and fiber respectively.

A. RADIO ACCESS

The received RF signal at the relay node, R_1, can be expressed as

$$y_{S,R1} = h_{S,R1}x + \sum_{i=1}^{M} h_i x_i + n_{R1} \tag{1}$$

where $h_{S,R1}$ is the fading RF channel coefficient, x is the modulation symbol, h_i is the fading RF channel coefficient for

the i^{th} interferer, x_i is the modulation symbol of the i^{th} interferer, and n_{R1} is an additive white Gaussian noise (AWGN) with variance σ^2_{R1} at the relay node, R_1. Both $h_{\text{S,R1}}$ and h_i are assumed to be Rayleigh distributed [23] and there are M RF co-channel interferers. We assume that $E\{y_{\text{S,R1}}\} = 0$ which is consistent with an ac-coupled RF channel.

B. FSO RELAY

To ensure that the received RF signal is unipolar in order to be able to drive the laser, a DC bias is added to the received signal after amplifying it at the first relay with a fixed gain G_1. Let P_{opt1} denote the emitted average optical power of the FSO relay node which is limited by eye-safety regulations. Since the radio signal is zero mean, the output signal will have an average optical power P_{opt1} as required. To consider the finite dynamic range of the laser driver, G_1 is selected to ensure that $\mid G_1 y_{\text{S,R1}} \mid \leq P_{\text{opt1}}$ with high probability to avoid over modulation induced clipping [8], [24]. Consider selecting G_1 to normalize the variance of the modulating signal. In particular, define G_1 as

$$G_1 = \frac{P_{\text{opt1}}}{K_1\sqrt{E\left[\mid h_{\text{S,R1}} \mid^2\right]P_{\text{RF}} + \sum_{i=1}^{M} E\left[\mid h_i \mid^2\right]P_{\text{Ri}} + \sigma^2_{\text{R}_1}}} \tag{2}$$

where P_{RF} and P_{Ri} are the average powers of the RF signal and the i^{th} RF interferer. The parameter K_1 is selected so that $2K_1$ standard deviations of the modulating signal are within the dynamic range of the modulator. Assuming Gaussian statistics, for $K_1 = 4$ the likelihood of clipping is on the order of 10^{-5}. Thus, when K_1 is chosen large enough, the impact of clipping in the laser driver of R_1 can be ignored.

Assuming direct analog modulation of the laser intensity at the relay node, R_1 and assuming that the electrical-to-optical conversion coefficient $\eta_1 = 1$, the retransmitted optical signal is

$$y_{R1\text{opt}} = P_{\text{opt1}} + G_1\, y_{\text{S,R1}}. \tag{3}$$

C. FIBER BACKHAUL LINK

The received electrical signal at the relay node, R_2, after removing the DC bias is given by

$$y_{\text{R1,R2}} = \mathcal{R}_1\, h_{\text{R1,R2}} G_1\, y_{\text{S,R1}} + n_{\text{R2}} \tag{4}$$

where $\mathcal{R}_1$ is the responsivity of the photodiode (PD) at the relay node, R_2, $h_{\text{R1,R2}}$ is the fading FSO irradiance fluctuations and n_{R_2} is AWGN added at relay node R_2 with variance σ^2_{R2}.

After amplifying the received signal at the second relay with a fixed gain G_2, a DC bias is added to be able to drive the laser. Similar to the case in relay R_1,

$$G_2 = \frac{P_{\text{opt2}}}{K_2\sqrt{\frac{\mathcal{R}_1^2\, E[|h_{\text{R1,R2}}|^2]P^2_{\text{opt1}}}{K_1^2} + \sigma^2_{\text{R2}}}} \tag{5}$$

where P_{opt2} is the average launched optical power in the single-mode fiber (SMF) per channel and K_2 is selected to control the likelihood of clipping by the laser driver. Considering an electrical-to-optical conversion coefficient $\eta_2 = 1$ and K_2 large enough, the optical signal forwarded into the fiber is

$$y_{\text{R2opt}} = P_{\text{opt2}} + G_2\, y_{\text{R1,R2}}. \tag{6}$$

Following the GN model [17], the impairments caused by the fiber nonlinear interference can be considered as an additive Gaussian noise n_{NLI} of power P_{NLI} that is statistically independent from the transmitted signal [17], [18], [20], [21]. Since a photodetector responds to the optical intensity, at node D, and assuming that the fiber loss is compensated by an electrical amplifier, the received electrical signal is

$$\begin{aligned} y_{\text{R2,D}} &= \mathcal{R}_2\left|\sqrt{y_{\text{R2opt}}} + n_{\text{NLI}}\right|^2 + n_{\text{D}} \\ &= \mathcal{R}_2\left(y_{\text{R2opt}} + n^2_{\text{NLI}} + 2n_{\text{NLI}}\sqrt{y_{\text{R2opt}}}\right) + n_{\text{D}} \end{aligned} \tag{7}$$

where $\mathcal{R}_2$ is the responsivity of the photodiode and n_{D} is AWGN with variance σ^2_{D} added in electrical domain at D. After removing the DC bias, the received electrical signal can be written as

$$y_{\text{R2,D}} = \mathcal{R}_2\left(G_2\, y_{\text{R1,R2}} + n^2_{\text{NLI}} + 2n_{\text{NLI}}\sqrt{y_{\text{R2opt}}}\right) + n_{\text{D}}. \tag{8}$$

Under a worst case assumption, P_{NLI} is set according to the maximum allowed launched optical power ($2P_{\text{opt2}}$). In this case, the nonlinear interference variance is given by [17]–[22]

$$P_{\text{NLI}} = \frac{\gamma^2_{\text{nl}}}{\pi|\beta_2|}\frac{L^2_{\text{eff}}}{L_{\text{eff,a}}}\frac{(2P_{\text{opt2}})^3}{B^2_{\text{ch}}}\text{arcsinh}\left(\frac{3}{8}\pi^2 L_{\text{eff,a}}|\beta_2|B^2_{\omega}\right) \tag{9}$$

where $L_{\text{eff}} = (1 - e^{-2\alpha_f L})/2\alpha_f$ and $L_{\text{eff,a}} = 1/2\alpha_f$ are the effective and asymptomatic-effective fiber lengths, respectively, for a fiber with a physical fiber length L and a SMF attenuation coefficient α_f. The total wavelength-division multiplexing (WDM) bandwidth is denoted $B_\omega = B_{\text{ch}}N_{\text{ch}}$, where N_{ch} is the number of WDM channels and B_{ch} is the fiber channel bandwidth. The group-velocity dispersion (GVD) is denoted β_2, and $\gamma_{\text{nl}} = 2\pi n_2/\lambda A_{\text{eff}}$ is the fiber nonlinearity coefficient, where A_{eff} is the core effective area, λ is the propagated wavelength, and n_2 is the nonlinear-index coefficient.

Notice from (8) that the noise term n^2_{NLI} has variance ($2P^2_{\text{NLI}}$) while the beating noise term $\left(2n_{\text{NLI}}\sqrt{y_{\text{R2opt}}}\right)$ has variance ($4P_{\text{opt2}}P_{\text{NLI}}$). In practice the impact of the beating noise term dominates and, using the parameters in Sec. VI, its power is at least about 3 orders of magnitude larger than the power of n^2_{NLI}. Thus, in the following the impact of n^2_{NLI} is removed from the channel model in (8) yielding

$$y_{\text{R2,D}} = \mathcal{R}_2\left(G_2\, y_{\text{R1,R2}} + 2n_{\text{NLI}}\sqrt{y_{\text{R2opt}}}\right) + n_{\text{D}}. \tag{10}$$

The beating noise term is also modelled as having a Gaussian distribution which can be shown to be a good fit for the power ranges considered in this work.

D. OVERALL SIGNAL-TO-INTERFERENCE-PLUS-NOISE RATIO

The overall signal-to-interference-plus-noise ratio (SINR) of the radio access link and the FSO/fiber backhaul at node D, γ_T, can be written in terms of the SNRs of each portion of the relay network as

$$\gamma_T = \frac{\gamma_1 \gamma_2}{\gamma_2 + \gamma_2 \gamma_R + C_1^2 (1 + C_2^2/\gamma_3)} \tag{11}$$

where

$$\begin{aligned}
\gamma_1 &= \frac{|\, h_{S,R1} \,|^2 \, P_{RF}}{\sigma_{R1}^2} \\
\gamma_R &= \sum_{i=1}^{M} \gamma_{Ri} = \frac{\sum_{i=1}^{M} |\, h_i \,|^2 \, P_{Ri}}{\sigma_{R1}^2} \\
\gamma_2 &= \frac{\mathcal{R}_1^2 \, |\, h_{R1,R2} \,|^2 \, P_{opt1}^2}{\sigma_{R2}^2} \\
\gamma_3 &= \frac{\mathcal{R}_2^2 P_{opt2}^2}{4\mathcal{R}_2^2 P_{opt2} P_{NLI} + \sigma_D^2} \\
C_1 &= K_1 \sqrt{\overline{\gamma_1} + \sum_{i=1}^{M} \overline{\gamma_{Ri}} + 1} \\
C_2 &= K_2 \sqrt{\frac{\overline{\gamma_2}}{K_1^2} + 1}
\end{aligned} \tag{12}$$

and where γ_1, γ_R, γ_2, and γ_3 are the instantaneous SNR of the RF link, the instantaneous overall interference-to-noise ratio (INR) of the RF link, the instantaneous electrical SNR of the FSO link, and the electrical SNR of the fiber link, respectively. Notice that γ_3 is deterministic under the condition of the worst case fiber nonlinear interference. The notation $\overline{\gamma_k}$ denotes the expected value of SNR, i.e, $E\{\gamma_k\}$.

E. CHANNEL STATISTICS

The RF link (i.e. S-R_1 link) is assumed to experience Rayleigh fading and hence γ_1 is exponentially distributed [23]

$$f_{\gamma_1}(\gamma_1) = \frac{1}{\overline{\gamma_1}} \exp\left(\frac{-\gamma_1}{\overline{\gamma_1}}\right). \tag{13}$$

It is known that the distribution of the sum of M independent and identically distributed equal power exponential random variables (RVs) is gamma distribution [25]. Then, $\gamma_R = \sum_{i=1}^{M} \gamma_{Ri}$ follows gamma distribution, where γ_{Ri} is the instantaneous INR of the i^{th} interferer, with distribution

$$f_{\gamma_R}(\gamma_R) = \frac{\gamma_R^{M-1}}{\overline{\gamma_{Ri}}^{M} \Gamma(M)} \exp\left(\frac{-\gamma_R}{\overline{\gamma_{Ri}}}\right) \tag{14}$$

where $\Gamma(.)$ is the gamma function.

The FSO link (i.e. R_1-R_2 link) is assumed to have gamma-gamma fading with pointing error impairments. The distribution of γ_2 is [15], [26]

$$f_{\gamma_2}(\gamma_2) = \frac{\zeta^2}{2\Gamma(\alpha)\Gamma(\beta)\gamma_2} G_{1,3}^{3,0}\left(E\alpha\beta\sqrt{\frac{\gamma_2}{\mu_2}} \,\middle|\, \begin{matrix} \zeta^2+1 \\ \zeta^2, \alpha, \beta \end{matrix}\right) \tag{15}$$

where $\mu_2 = \frac{\overline{\gamma_2}\alpha\beta\zeta^2(\zeta^2+2)}{(\alpha+1)(\beta+1)(\zeta^2+1)^2}$, $E = \frac{\zeta^2}{\zeta^2+1}$, ζ is the ratio between the equivalent beam radius at the receiver and the pointing error displacement standard deviation at the receiver [27], $G(\cdot)$ is the Meijer G function [28], and α and β are the scintillation parameters [29]

$$\alpha = \left(\exp\left[\frac{0.49\sigma_R^2}{\left(1 + 1.11\sigma_R^{\frac{12}{5}}\right)^{\frac{7}{6}}} \right] - 1 \right)^{-1} \tag{16}$$

$$\beta = \left(\exp\left[\frac{0.51\sigma_R^2}{\left(1 + 0.69\sigma_R^{\frac{12}{5}}\right)^{\frac{5}{6}}} \right] - 1 \right)^{-1} \tag{17}$$

where $\sigma_R^2 = 1.23 C_n^2 (2\pi/\lambda)^{\frac{7}{6}} L_{FSO}^{\frac{11}{6}}$ is unitless Rytov variance, C_n^2 is the refractive-index structure parameter, and L_{FSO} is the FSO propagation distance.

III. OUTAGE PROBABILITY AND CAPACITY-CDF ANALYSIS

The outage probability of the AF relayed FSO/fiber backhauled system is defined as

$$\begin{aligned}
P_{out}(\gamma_{th}) &= Pr[\gamma_T < \gamma_{th}] \\
&= Pr\left[\frac{\gamma_1\gamma_2}{\gamma_2 + \gamma_2\gamma_R + C_1^2(1+C_2^2/\gamma_3)} < \gamma_{th}\right]
\end{aligned} \tag{18}$$

where γ_{th} is the threshold on overall SINR that guarantees a minimum level of link quality. Substituting distributions from Sec. II-E yields

$$\begin{aligned}
&P_{out}(\gamma_{th}) \\
&= \int_0^\infty \int_0^\infty Pr\left[\gamma_1 < \gamma_{th} \frac{\gamma_2 + \gamma_2\gamma_R + C_1^2(1 + C_2^2/\gamma_3)}{\gamma_2}\right] \\
&\qquad \times f_{\gamma_R}(\gamma_R) f_{\gamma_2}(\gamma_2) d\gamma_R d\gamma_2 \\
&= 1 - \int_0^\infty \int_0^\infty \exp\left(-\gamma_{th} \frac{\gamma_2 + \gamma_2\gamma_R + C_1^2(1 + C_2^2/\gamma_3)}{\overline{\gamma_1}\gamma_2}\right) \\
&\qquad \times f_{\gamma_R}(\gamma_R) f_{\gamma_2}(\gamma_2) d\gamma_R d\gamma_2.
\end{aligned} \tag{19}$$

Using [28, eq. (3.351.3)], the last integration can be written as

$$\begin{aligned}
P_{out}(\gamma_{th}) = 1 &- \left(1 + \frac{\gamma_{th}\overline{\gamma_{Ri}}}{\overline{\gamma_1}}\right)^{-M} \exp\left(\frac{-\gamma_{th}}{\overline{\gamma_1}}\right) \\
&\times \int_0^\infty \exp\left(\frac{-\gamma_{th} C_1^2 (1 + C_2^2/\gamma_3)}{\overline{\gamma_1}\gamma_2}\right) f_{\gamma_2}(\gamma_2) d\gamma_2.
\end{aligned} \tag{20}$$

By expressing $\exp\left(\frac{-\gamma_{th} C_1^2(1+C_2^2/\gamma_3)}{\overline{\gamma_1}\gamma_2}\right)$ in terms of the Meijer G function using [30, eq. (07.34.03.0046.01)], the last

integration can be written as

$$P_{\text{out}}(\gamma_{\text{th}}) = 1 - \left(1 + \frac{\gamma_{\text{th}}\overline{\gamma_{\text{Ri}}}}{\overline{\gamma_{\text{I}}}}\right)^{-M} \exp\left(\frac{-\gamma_{\text{th}}}{\overline{\gamma_{\text{I}}}}\right) \frac{\zeta^2}{2\Gamma(\alpha)\Gamma(\beta)} \times \int_0^\infty \gamma_2^{-1} G_{1,0}^{0,1}\left(\frac{\overline{\gamma_{\text{I}}}\gamma_2}{\gamma_{\text{th}} C_1^2(1+C_2^2/\gamma_3)}\middle| \begin{matrix}1\\-\end{matrix}\right) \times G_{1,3}^{3,0}\left(E\alpha\beta\sqrt{\frac{\gamma_2}{\mu_2}}\middle| \begin{matrix}\zeta^2+1\\ \zeta^2, \alpha, \beta\end{matrix}\right) d\gamma_2. \quad (21)$$

Using [31, eq. (21)] and [30, eqs. (07.34.04.0003.01), (07.34.04.0004.01), and (07.34.03.0002.01)], P_{out} can be written more compactly as

$$P_{\text{out}}(\gamma_{\text{th}}) = 1 - \frac{2^{\alpha+\beta}\zeta^2}{8\pi\Gamma(\alpha)\Gamma(\beta)}\left(1+\frac{\gamma_{\text{th}}\overline{\gamma_{\text{Ri}}}}{\overline{\gamma_{\text{I}}}}\right)^{-M} \exp\left(\frac{-\gamma_{\text{th}}}{\overline{\gamma_{\text{I}}}}\right) \times G_{1,6}^{6,0}\left(\frac{(E\alpha\beta)^2\gamma_{\text{th}}C_1^2(1+C_2^2/\gamma_3)}{16\overline{\gamma_{\text{I}}}\mu_2}\middle| \begin{matrix}a\\ b\end{matrix}\right) \quad (22)$$

where $a \overset{\text{def}}{=} \left\{\frac{\zeta^2}{2}+1\right\}$ and $b \overset{\text{def}}{=} \left\{\frac{\zeta^2}{2}, \frac{\alpha}{2}, \frac{\alpha+1}{2}, \frac{\beta}{2}, \frac{\beta+1}{2}, 0\right\}$.

As another performance metric, the CDF of end user capacity using mixed FSO/fiber backhaul system can be computed in a similar manner. The capacity of the overall system in bits per second can be estimated as [32]

$$C = R_{\text{s}} \log_2(1+\gamma_{\text{T}}) \quad (23)$$

where R_{s} is the symbol rate. The CDF of user capacity takes the form

$$F_{\text{C}}(C_0) = Pr\left[R_{\text{s}}\log_2(1+\gamma_{\text{T}}) < C_0\right] = Pr\left[\gamma_{\text{T}} < 2^{(C_0/R_{\text{s}})} - 1\right] \quad (24)$$

for some target capacity C_0. Using (22) and replacing γ_{th} with $\left(2^{(C_0/R_{\text{s}})} - 1\right)$ yields $F_{\text{C}}(C_0)$.

IV. AVERAGE BER ANALYSIS

Using [33, eq. (12)], the average user BER using mixed FSO/fiber backhaul systems for a variety of binary modulations can be obtained as

$$\overline{BER} = \frac{q^p}{2\Gamma(p)}\int_0^\infty \exp(-q\gamma_{\text{th}})\gamma_{\text{th}}^{p-1} P_{\text{out}}(\gamma_{\text{th}}) d\gamma_{\text{th}} \quad (25)$$

where p and q account for different modulation techniques. Expressing $\left(1+\frac{\gamma_{\text{th}}\overline{\gamma_{\text{Ri}}}}{\overline{\gamma_{\text{I}}}}\right)^{-M}$ in terms of Meijer G function [30, eq. (07.34.03.0271.01)], and substituting (22) into (25) gives

$$\overline{BER} = \frac{1}{2} - \frac{2^{\alpha+\beta}\zeta^2 q^p}{16\pi\Gamma(\alpha)\Gamma(\beta)\Gamma(p)\Gamma(M)}\int_0^\infty \gamma_{\text{th}}^{p-1} \times \exp\left(-\left(q+\frac{1}{\overline{\gamma_{\text{I}}}}\right)\gamma_{\text{th}}\right) G_{1,1}^{1,1}\left(\frac{\overline{\gamma_{\text{Ri}}}}{\overline{\gamma_{\text{I}}}}\gamma_{\text{th}}\middle| \begin{matrix}1-M\\ 0\end{matrix}\right) \times G_{1,6}^{6,0}\left(\frac{(E\alpha\beta)^2\gamma_{\text{th}}C_1^2(1+C_2^2/\gamma_3)}{16\overline{\gamma_{\text{I}}}\mu_2}\middle| \begin{matrix}a\\ b\end{matrix}\right) d\gamma_{\text{th}}. \quad (26)$$

Using [33, eqs. (14) and (20) and Table I], the last integration can be written as

$$\overline{BER} = \frac{1}{2} - \frac{2^{\alpha+\beta}\zeta^2 q^p}{16\pi\Gamma(\alpha)\Gamma(\beta)\Gamma(p)\Gamma(M)\left(q+\frac{1}{\overline{\gamma_{\text{I}}}}\right)^p} \times G_{1,0:1,1:6,0}^{1,0:1,1:6,0}\left(\begin{matrix}p\\-\end{matrix}\middle| \begin{matrix}1-M\\0\end{matrix}\middle| \begin{matrix}a\\b\end{matrix}\middle| \frac{\overline{\gamma_{\text{Ri}}}}{(1+q\overline{\gamma_{\text{I}}})}, \frac{(E\alpha\beta)^2 C_1^2(1+C_2^2/\gamma_3)}{16\mu_2(1+q\overline{\gamma_{\text{I}}})}\right) \quad (27)$$

where $G_{\cdot,\cdot:\cdot,\cdot:\cdot,\cdot}^{\cdot,\cdot:\cdot,\cdot:\cdot,\cdot}\left(\cdot\middle|\cdot\middle|\cdot\middle|\cdot,\cdot\right)$ is the extended generalized bivariate Meijer G function (EGBMGF) [33]. The EGBMGF is efficiently implemented in a variety of commercial mathematics software (e.g., [33], [34]).

For the interference free case ($M = 0$), a simpler expression for $\overline{BER}$ is (following a similar approach as [7, eq. (14)])

$$\overline{BER_0} = \frac{1}{2} - \frac{2^{\alpha+\beta}\zeta^2 q^p}{16\pi\Gamma(\alpha)\Gamma(\beta)\Gamma(p)\left(q+\frac{1}{\overline{\gamma_{\text{I}}}}\right)^p} \times G_{2,6}^{6,1}\left(\frac{(E\alpha\beta)^2 C_1^2(1+C_2^2/\gamma_3)}{16\mu_2(q\overline{\gamma_{\text{I}}}+1)}\middle| \begin{matrix}1-p, a\\ b\end{matrix}\right). \quad (28)$$

V. ASYMPTOTIC ANALYSIS

In order to provide greater physical insights, in this section the asymptotic outage probability and average BER expressions at high SNR regime are derived and used to compute the optimum fiber average launched power.

A. ASYMPTOTIC OUTAGE AND BER

In (22), the Meijer G function makes additional analytical derivations difficult. In the case of large $\overline{\gamma_2}$ and γ_3 the following approximation can be applied [30, eq. (07.34.06.0006.01)]

$$G_{1,6}^{6,0}\left(\frac{(E\alpha\beta)^2\gamma_{\text{th}}C_1^2(1+C_2^2/\gamma_3)}{16\overline{\gamma_{\text{I}}}\mu_2}\middle| \begin{matrix}a\\b\end{matrix}\right) \approx G(\gamma_{\text{th}}) = \sum_{k=1}^{6}\frac{\prod_{j=1, j\neq k}^{6}\Gamma(b_j-b_k)}{\Gamma(a-b_k)}\left(\frac{(E\alpha\beta)^2\gamma_{\text{th}}C_1^2(1+C_2^2/\gamma_3)}{16\overline{\gamma_{\text{I}}}\mu_2}\right)^{b_k}. \quad (29)$$

In Fig. 2, the Meijer G function in (29) and its approximation, $G(\gamma_{\text{th}})$, are plotted versus P_{opt2} at high $\overline{\gamma_2}$ for different turbulence and pointing error conditions levels. Initially as P_{opt2} increases, γ_3 becomes high and so the approximation is tight. This is true as long as the fiber nonlinearity noise is low and not dominant. However, at high values of P_{opt2}, γ_3 is reduced due to fiber nonlinearity noise. Thus there is a range of P_{opt2} values over which this fit is tight as will be discussed in Sec. VI.

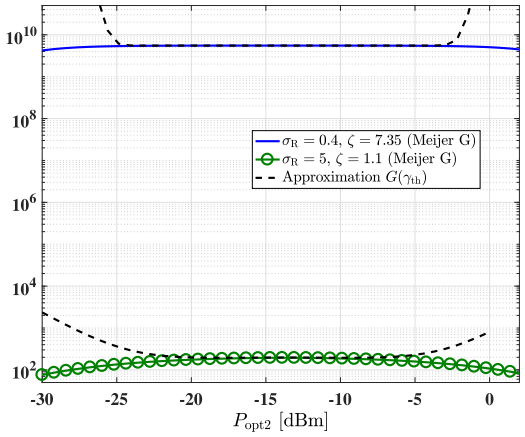

FIGURE 2. Approximation $G(\gamma_{th})$ versus P_{opt2} ($M = 0$, $\gamma_{th} = 0$ dB, and $\overline{\gamma_2} = 70$ dB).

For a fixed and finite $\overline{\gamma_1}$, the asymptotic outage probability at high $\overline{\gamma_2}$ and γ_3 is

$$P_{\text{out}}^{\text{asym}}(\gamma_{\text{th}}) = 1 - \frac{2^{\alpha+\beta}\zeta^2}{8\pi\Gamma(\alpha)\Gamma(\beta)}\left(1+\frac{\gamma_{\text{th}}\overline{\gamma_{\text{Ri}}}}{\overline{\gamma_1}}\right)^{-M}\exp\left(\frac{-\gamma_{\text{th}}}{\overline{\gamma_1}}\right) \times \sum_{k=1}^{6}\frac{\prod_{j=1,j\neq k}^{6}\Gamma(b_j-b_k)}{\Gamma(a-b_k)}\left(\frac{(E\alpha\beta)^2\,\gamma_{\text{th}}C_1^2(1+C_2^2/\gamma_3)}{16\overline{\gamma_1}\mu_2}\right)^{b_k}. \quad (30)$$

The asymptotic CDF of user capacity can be similarly derived.

Substituting (30) into (25) yields,

$$\overline{BER}^{\text{asym}} = \frac{1}{2} - \frac{2^{\alpha+\beta}\zeta^2 q^p}{16\pi\Gamma(\alpha)\Gamma(\beta)\Gamma(p)}\sum_{k=1}^{6}\frac{\prod_{j=1,j\neq k}^{6}\Gamma(b_j-b_k)}{\Gamma(a-b_k)} \times \left(\frac{(E\alpha\beta)^2\,C_1^2(1+C_2^2/\gamma_3)}{16\overline{\gamma_1}\mu_2}\right)^{b_k}\int_0^{\infty}\gamma_{\text{th}}^{b_k+p-1} \times \exp\left(-\gamma_{\text{th}}\left(q+\frac{1}{\overline{\gamma_1}}\right)\right)\left(1+\frac{\gamma_{\text{th}}\overline{\gamma_{\text{Ri}}}}{\overline{\gamma_1}}\right)^{-M}d\gamma_{\text{th}}. \quad (31)$$

Simplifying using [35, eq. (27)] gives

$$\overline{BER}^{\text{asym}} = \frac{1}{2} - \frac{2^{\alpha+\beta}\zeta^2 q^p}{16\pi\Gamma(\alpha)\Gamma(\beta)\Gamma(p)}\sum_{k=1}^{6}\frac{\prod_{j=1,j\neq k}^{6}\Gamma(b_j-b_k)}{\Gamma(a-b_k)} \times \left(\frac{(E\alpha\beta)^2\,C_1^2(1+C_2^2/\gamma_3)}{16\overline{\gamma_1}\mu_2}\right)^{b_k}\Gamma(b_k+p)\left(\frac{\overline{\gamma_1}}{\overline{\gamma_{Ri}}}\right)^{b_k+p} \times \Psi\left(b_k+p, b_k+p-M+1; \frac{(q\overline{\gamma_1}+1)}{\overline{\gamma_{\text{Ri}}}}\right) \quad (32)$$

where $\Psi(.,.;.)$ is the Tricomi confluent hypergeometric function [28, eq. (9.210.2)].

For the interference free case (i.e., $M = 0$), a simpler expression can be obtained for $\overline{BER}^{\text{asym}}$ using $G(\gamma_{\text{th}})$ as

$$\overline{BER_0}^{\text{asym}} = \frac{1}{2} - \frac{2^{\alpha+\beta}\zeta^2 q^p}{16\pi\Gamma(\alpha)\Gamma(\beta)\Gamma(p)\left(q+\frac{1}{\overline{\gamma_1}}\right)^p} \times \sum_{k=1}^{6}\frac{\prod_{j=1,j\neq k}^{6}\Gamma(b_j-b_k)\Gamma(p+b_k)}{\Gamma(a-b_k)} \times \left(\frac{(E\alpha\beta)^2\,C_1^2(1+C_2^2/\gamma_3)}{16\mu_2\,(q\overline{\gamma_1}+1)}\right)^{b_k}. \quad (33)$$

B. OPTIMUM FIBER AVERAGE LAUNCHED POWER P_{opt2}^*

Due to the fiber channel, the average launched power must be carefully selected to balance the impacts of receiver noise and the inherent nonlinearity of the channel.

Let P_{opt2}^* denote the optimum average launched fiber optical power which minimizes outage. Consider setting the first derivative of $P_{\text{out}}^{\text{asym}}$ in (30) with respect to P_{opt2} to zero,

$$\frac{\partial P_{\text{out}}^{\text{asym}}}{\partial P_{\text{opt2}}} = -\frac{2^{\alpha+\beta}\zeta^2 C_2^2}{8\pi\Gamma(\alpha)\Gamma(\beta)}\left(1+\frac{\gamma_{\text{th}}\overline{\gamma_{\text{Ri}}}}{\overline{\gamma_1}}\right)^{-M}\exp\left(\frac{-\gamma_{\text{th}}}{\overline{\gamma_1}}\right) \times \sum_{k=1}^{6}\frac{\prod_{j=1,j\neq k}^{6}\Gamma(b_j-b_k)}{\Gamma(a-b_k)}\left(\frac{(E\alpha\beta)^2\,\gamma_{\text{th}}C_1^2}{16\overline{\gamma_1}\mu_2}\right)^{b_k} \times b_k\left(1+\frac{C_2^2\sigma_D^2}{\mathcal{R}_2^2P_{\text{opt2}}^2}+4C_2^2C_{\text{NLI}}P_{\text{opt2}}^2\right)^{b_k-1} \times \left(\frac{-2\sigma_D^2}{\mathcal{R}_2^2P_{\text{opt2}}^3}+8C_{\text{NLI}}P_{\text{opt2}}\right)=0 \quad (34)$$

where $C_{\text{NLI}} = P_{\text{NLI}}/P_{\text{opt2}}^3$. After some simplification, the optimal P_{opt2} can be written as

$$P_{\text{opt2}}^* = \left(\frac{\pi\sigma_D^2|\beta_2|L_{\text{eff,a}}B_{\text{ch}}^2}{32\mathcal{R}_2^2\gamma_{\text{nl}}^2\,L_{\text{eff}}^2\,\text{arcsinh}\left(\frac{3}{8}\pi^2L_{\text{eff,a}}|\beta_2|B_\omega^2\right)}\right)^{\frac{1}{4}}. \quad (35)$$

Note that P_{opt2}^* does not depend on $\overline{\gamma_1}$, $\overline{\gamma_{\text{Ri}}}$ nor $\overline{\gamma_2}$ under the condition of the worst case fiber nonlinearity interference scenario. It worth mentioning that P_{opt2}^* in (35) can also be obtained using the first derivative of (32) or (33).

VI. NUMERICAL RESULTS

The analytic expressions for the performance of the mixed FSO/fiber backhaul system are studied in this section to quantify the tightness of the asymptotic results and to reveal approaches for the design of such systems. The parameters for the SMF used in the backhaul network are given in Table 1 [18]. Though in this study we consider a single

TABLE 1. Parameters of fiber Backhaul link.

Parameter	Symbol	Value
Physical SMF length	L	10 km
SMF attenuation coefficient	α_f	0.22 dB/km
SMF dispersion coefficient	D	16.7 ps/km.nm
SMF nonlinearity coefficient	$\gamma_{\rm nl}$	1.3 $\rm W^{-1}km^{-1}$
SMF channel bandwidth	$B_{\rm ch}$	32 GHz
The number of WDM channels	$N_{\rm ch}$	1
Detector Noise	$\sigma_{\rm D}^2$	10^{-14} $\rm A^2$

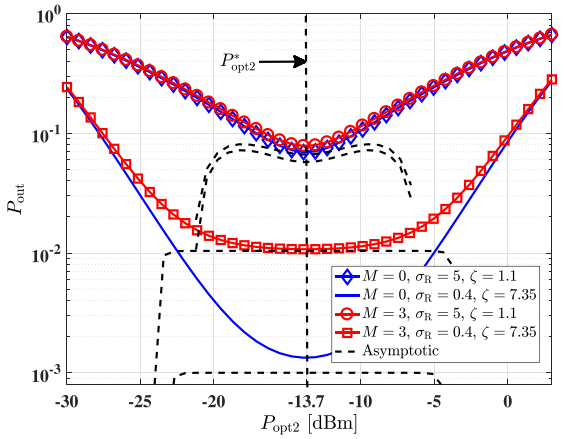

FIGURE 3. $P_{\rm out}$ **versus** $P_{\rm opt2}$ **(**$\gamma_{\rm th}$ **= 0 dB,** $\overline{\gamma_1}$ **= 30 dB,** $\overline{\gamma_2}$ **= 70 dB, and** $\overline{\gamma_{\rm Ri}}$ **= 5 dB).**

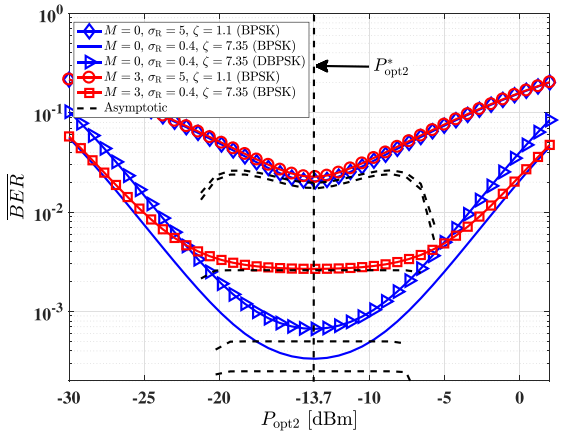

FIGURE 4. $\overline{BER}$ **versus** $P_{\rm opt2}$ **for different modulation techniques (**$\gamma_{\rm th}$ **= 0 dB,** $\overline{\gamma_1}$ **= 30 dB,** $\overline{\gamma_2}$ **= 70 dB, and** $\overline{\gamma_{\rm Ri}}$ **= 5 dB) (**$p = 0.5$ **and** $q = 1$ **for BPSK and** $p = 1$ **and** $q = 1$ **for DBPSK [33]).**

WDM channel, in practice multiple FSO receptions can be multiplexed on a single or over multiple WDM channels. Without loss of generality, the responsivities $\mathcal{R}_1 = \mathcal{R}_2 = 1$ are assumed. Given the variability of the RF and FSO channels, performance will be studied for a variety of SNR values, turbulence strengths and pointing error severity.

Figures 3 and 4 show the outage probability (22) and the average BER, computed in (27) and (28), versus $P_{\rm opt2}$ with different values for the average overall RF access network

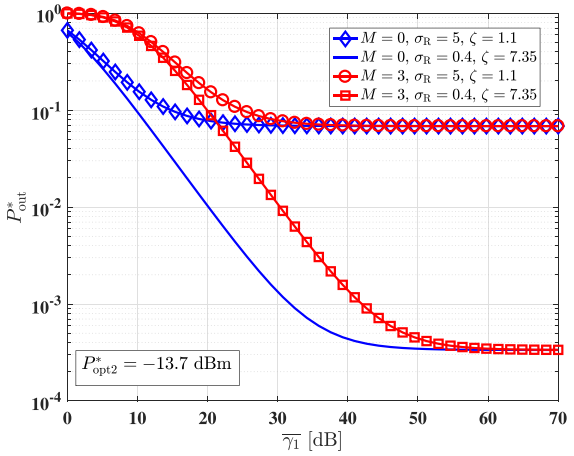

FIGURE 5. $P^*_{\rm out}$ **versus** $\overline{\gamma_1}$ **for different FSO conditions and RF interferers (**$\gamma_{\rm th}$ **= 0 dB,** $\overline{\gamma_2}$ **= 70 dB, and** $\overline{\gamma_{\rm Ri}}$ **= 5 dB,** $P_{\rm opt2} = P^*_{\rm opt2}$**).**

INR, FSO pointing error, and turbulence strength levels. In all cases, there is an optimal value for the average launched fiber power which maximizes performance. If $P_{\rm opt2} > P^*_{\rm opt2} \approx -13.7$ dBm (computed via (35)), fiber nonlinearity dominates limiting the system performance. Notice also that the asymptotic results, from (30), (32) and (33), are only tight near $P^*_{\rm opt2}$ when γ_3 is large enough to make the approximation valid. Furthermore, the addition of RF co-channel interference in the access network degrades performance, as expected. An interesting feature is that in the presence of co-channel interference in the RF access network, the performance flattens near $P^*_{\rm opt2}$. This phenomenon occurs because the RF co-channel interferers dominate over the backhaul impairments of both FSO and fiber links. However, in worse FSO channel conditions, optical fading and pointing errors dominate and the impact of co-channel interferers is not as significant. In the case of no co-channel interferers, the curves do not flatten near $P^*_{\rm opt2}$ and the system performance is greatly improved for good FSO channel conditions.

The minimum outage probability ($P^*_{\rm out}$), computed at $P^*_{\rm opt2}$, is plotted versus $\overline{\gamma_1}$ and $\overline{\gamma_2}$ in Figs. 5 and 6, respectively. As expected, by increasing $\overline{\gamma_1}$ or $\overline{\gamma_2}$, $P^*_{\rm out}$ improves. Similarly, as the number of interferers increase or the weather and the pointing error conditions become worse, $P^*_{\rm out}$ degrades. In addition, at high $\overline{\gamma_1}$ or $\overline{\gamma_2}$, $P^*_{\rm out}$ saturates. This saturation in performance is due to the selection of G_1 (2) and G_2 (5) to control the clipping distortion and to ensure non-negativity of the signal inputted to the optical intensity modulator. In this work $K_1 = K_2 = 4$ and are fixed to model a simple automatic gain control system which is already available in many commercial FSO systems [36].

Notice in Fig. 5, that $P^*_{\rm out}$ saturates at a lower $\overline{\gamma_1}$ when FSO conditions are worse due to the dominance of the FSO impairments. Furthermore, in Fig. 6, for good FSO conditions, the system performance saturates at a lower $\overline{\gamma_2}$ after adding the RF co-channel interference due to the dominance of the RF impairments. However, for worse FSO channel conditions, the RF co-channel interference has little impact.

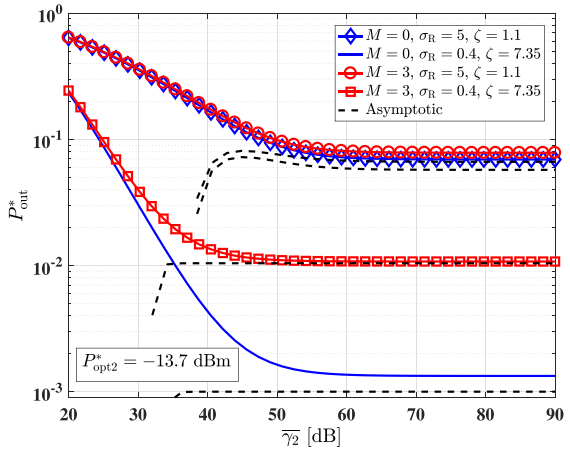

FIGURE 6. P^*_{out} versus $\overline{\gamma_2}$ for different FSO conditions and RF interferers ($\gamma_{th} = 0$ dB, $\overline{\gamma_I} = 30$ dB, and $\overline{\gamma_{Ri}} = 5$ dB, $P_{opt2} = P^*_{opt2}$).

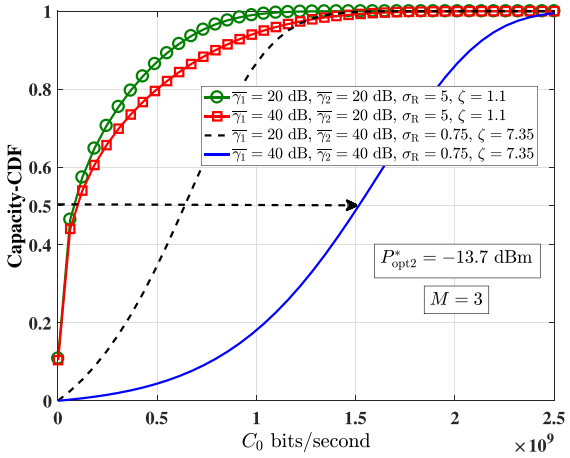

FIGURE 7. CDF of the estimated user capacity for different RF and FSO backhaul conditions ($\overline{\gamma_{Ri}} = 5$ dB and $R_s = 220$ Msymbols/sec, $P_{opt2} = P^*_{opt2}$).

In Fig. 7, the CDF of the estimated user capacity is plotted at P^*_{opt2}, for different $\overline{\gamma_I}$ and $\overline{\gamma_2}$, using mm-wave RF access with $R_s = 220$ Msymbols/sec [2]. The distribution of user rates is impacted by both RF and FSO channels, however, they are much more sensitive to the FSO backhaul conditions. When the FSO channel is poor, $\overline{\gamma_I}$ has little impact on system performance. However, in good FSO conditions, the RF SNR greatly impacts user rates. In particular, the 50-th percentile user rates can reach 1.5 Gbits/sec under favorable RF and FSO conditions.

VII. CONCLUSION

In this paper, we present analytical results quantifying the performance of 5G RF access networks with a mixed AF FSO and fiber backhaul. In the access network, the impact of RF co-channel interferers is considered while in the backhaul the impact of FSO pointing errors, fiber nonlinearity as well as the limited dynamic range of optical emitters are modelled. Under fixed gain relaying, closed-form and asymptotic expressions for the outage probability, the average BER, and the CDF of end user capacity of the mixed FSO/fiber backhaul systems are derived. Our results reveal that there is an optimal average launched optical power into the fiber which balances the impact of improving received signal power with the distortion of fiber nonlinearity. In the region above the optimal fiber average launched power, increasing the optical average launched power yields more outage because of the dominance of the fiber nonlinearity. A key conclusion that is quantified in this work is that the quality of the variable FSO backhaul channel has a dominating impact on the user rates as compared to the RF access channel (when transmitting at optimum fiber average launched power P^*_{opt2}). This work thus serves as a tool to help in the planning and provisioning of the 5G networks with FSO and fiber backhaul components.

REFERENCES

[1] X. Ge, S. Tu, G. Mao, and C. X. Wang, "5G ultra-dense cellular networks," *IEEE Trans. Wireless Commun.*, vol. 23, no. 1, pp. 72–79, Feb. 2016.

[2] C. Dehos, J. L. González, A. D. Domenico, D. Ktenas, and L. Dussopt, "Millimeter-wave access and backhauling: The solution to the exponential data traffic increase in 5G mobile communications systems?" *IEEE Commun. Mag.*, vol. 52, no. 9, pp. 88–95, Sep. 2014.

[3] R. K. Al-Dabbagh and H. S. Al-Raweshidy, "64-GHz millimeter-wave photonic generation with a feasible radio over fiber system," *Opt. Eng.*, vol. 56, no. 2, pp. 026117–1–026117–10, Feb. 2017.

[4] P. V. Trinh, T. C. Thang, and A. T. Pham, "Mixed mmWave RF/FSO relaying systems over generalized fading channels with pointing errors," *IEEE Photon. J.*, vol. 9, no. 1, Feb. 2017, Art. no. 5500414.

[5] E. Soleimani-Nasab and M. Uysal, "Generalized performance analysis of mixed RF/FSO cooperative systems," *IEEE Trans. Wireless Commun.*, vol. 15, no. 1, pp. 714–727, Jan. 2016.

[6] E. Lee, J. Park, D. Han, and G. Yoon, "Performance analysis of the asymmetric dual-hop relay transmission with mixed RF/FSO links," *IEEE Photon. Technol. Lett.*, vol. 23, no. 21, pp. 1642–1644, Nov. 1, 2011.

[7] I. S. Ansari, F. Yilmaz, and M.-S. Alouini, "Impact of pointing errors on the performance of mixed RF/FSO dual-hop transmission systems," *IEEE Wireless Commun. Lett.*, vol. 2, no. 3, pp. 351–354, Jun. 2013.

[8] M. I. Petkovic, A. M. Cvetkovic, G. T. Djordjevic, and G. K. Karagiannidis, "Partial relay selection with outdated channel state estimation in mixed RF/FSO systems," *J. Lightw. Technol.*, vol. 33, no. 13, pp. 2860–2867, Jul. 1, 2015.

[9] M. I. Petkovic, "Performance analysis of mixed RF/FSO systems," in *Proc. 23rd Telecommun. Forum*, Belgrade, Serbia, Nov. 2015, pp. 293–300.

[10] M. I. Petkovic, A. M. Cvetkovic, G. T. Djordjevic, and G. K. Karagiannidis, "Outage performance of the mixed RF/FSO relaying channel in the presence of interference," *Wireless Pers. Commun.*, vol. 96, no. 2, pp. 1–16, Jun. 2017.

[11] H. Samimi and M. Uysal, "End-to-end performance of mixed RF/FSO transmission systems," *J. Opt. Commun. Netw.*, vol. 5, no. 11, pp. 1139–1144, Nov. 2013.

[12] E. Zedini, I. S. Ansari, and M.-S. Alouini, "Performance analysis of mixed Nakagami-*m* and gamma-gamma dual-hop FSO transmission systems," *IEEE Photon. J.*, vol. 7, no. 1, Feb. 2015, Art. no. 7900120.

[13] S. Anees and M. R. Bhatnagar, "Performance of an amplify-and-forward dual-hop asymmetric RF-FSO communication system," *J. Opt. Commun. Netw.*, vol. 7, no. 2, pp. 124–135, Feb. 2015.

[14] L. Kong, W. Xu, L. Hanzo, H. Zhang, and C. Zhao, "Performance of a free-space-optical relay-assisted hybrid RF/FSO system in generalized *M*-distributed channels," *IEEE Photon. J.*, vol. 7, no. 5, Oct. 2015, Art. no. 7903319.

[15] J. Zhang, L. Dai, Y. Zhang, and Z. Wang, "Unified performance analysis of mixed radio frequency/free-space optical dual-hop transmission systems," *J. Lightw. Technol.*, vol. 33, no. 11, pp. 2286–2293, Jun. 1, 2015.

[16] E. Zedini, H. Soury, and M.-S. Alouini, "On the performance analysis of dual-hop mixed FSO/RF systems," *IEEE Trans. Wireless Commun.*, vol. 15, no. 5, pp. 3679–3689, May 2016.
[17] P. Poggiolini, A. Carena, G. B. V. Curri, and F. Forghieri, "Analytical modeling of nonlinear propagation in uncompensated optical transmission links," *IEEE Photon. Technol. Lett.*, vol. 23, no. 11, pp. 742–744, Jun. 1, 2011.
[18] A. E. El-Fiqi, A. E. Morra, S. F. Hegazy, H. M. H. Shalaby, K. Kato, and S. S. A. Obayya, "Performance evaluation of hybrid DPSK-MPPM techniques in long-haul optical transmission," *Appl. Opt.*, vol. 55, no. 21, pp. 5614–5622, Jul. 2016.
[19] W. Shieh and X. Chen, "Information spectral efficiency and launch power density limits due to fiber nonlinearity for coherent optical OFDM systems," *IEEE Photon. J.*, vol. 3, no. 2, pp. 158–173, Apr. 2011.
[20] P. Poggiolini, G. Bosco, A. Carena, V. Curri, Y. Jiang, and F. Forghieri. (Sep. 2012). "A detailed analytical derivation of the GN model of nonlinear interference in coherent optical transmission systems." [Online]. Available: https://arxiv.org/abs/1209.0394
[21] P. Poggiolini, G. Bosco, A. Carena, V. Curri, Y. Jiang, and F. Forghieri, "The GN-model of fiber non-linear propagation and its applications," *J. Lightw. Technol.*, vol. 32, no. 4, pp. 694–721, Feb. 15, 2014.
[22] G. Bosco, P. Poggiolini, A. Carena, V. Curri, and F. Forghieri, "Analytical results on channel capacity in uncompensated optical links with coherent detection," *Opt. Exp.*, vol. 20, no. 17, pp. 19610–19611, Aug. 2012.
[23] M. K. Simon and M.-S. Alouini, *Digital Communication Over Fading Channels*. Hoboken, NJ, USA: Wiley, 2000.
[24] X. Song, F. Yang, and J. Cheng, "Subcarrier intensity modulated optical wireless communications in atmospheric turbulence with pointing errors," *IEEE/OSA J. Opt. Commun. Netw.*, vol. 5, no. 4, pp. 349–358, Apr. 2013.
[25] M. Evans, N. Hastings, and B. Peacock, *Statistical Distributions*, 3rd ed. Hoboken, NJ, USA: Wiley, 2000.
[26] E. Zedini, I. S. Ansari, and M.-S. Alouini, "Unified performance analysis of mixed line of sight RF-FSO fixed gain dual-hop transmission systems," in *Proc. IEEE Wireless Commun. Netw. Conf.*, New Orleans, LA, USA, Mar. 2015, pp. 46–51.
[27] A. A. Farid and S. Hranilovic, "Outage capacity optimization for free-space optical links with pointing errors," *J. Lightw. Technol.*, vol. 25, no. 7, pp. 1702–1710, Jul. 2007.
[28] I. S. Gradshteyn and I. M. Ryzhik, *Table of Integrals, Series, and Products*, A. Jeffrey and D. Zwillinger, Eds., 7th ed. San Diego, CA, USA: Academic, Mar. 2007.
[29] M. A. Al-Habash, L. C. Andrews, and R. L. Phillips, "Mathematical model for the irradiance probability density function of a laser beam propagating through turbulent media," *Opt. Eng.*, vol. 40, pp. 1554–1562, Aug. 2001.
[30] Wolfram. (2017). *The Wolfram Functions Site*. [Online]. Available: http://functions.wolfram.com
[31] V. S. Adamchik and O. I. Marichev, "The algorithm for calculating integrals of hypergeometric type functions and its realization in REDUCE system," in *Proc. Int. Symp. Symbol. Algebraic Comput.*, Tokyo, Japan, Aug. 1990, pp. 212–224.
[32] R. Essiambre, G. Kramer, P. J. Winzer, G. J. Foschini, and B. Goebel, "Capacity limits of optical fiber networks," *J. Lightw. Technol.*, vol. 28, no. 4, pp. 662–701, Feb. 15, 2010.
[33] I. S. Ansari, S. Al-Ahmadi, F. Yilmaz, M.-S. Alouini, and H. Yanikomeroglu, "A new formula for the BER of binary modulations with dual-branch selection over generalized-K composite fading channels," *IEEE Trans. Commun.*, vol. 59, no. 10, pp. 2654–2658, Oct. 2011.
[34] H. Chergui, M. Benjillali, and S. Saoudi, "Performance analysis of project-and-forward relaying in mixed MIMO-pinhole and Rayleigh dual-hop channel," *IEEE Commun. Lett.*, vol. 20, no. 3, pp. 610–613, Mar. 2016.
[35] E. Soleimani-Nasab, M. Matthaiou, M. Ardebilipour, and G. Karagiannidis, "Two-way AF relaying in the presence of co-channel interference," *IEEE Trans. Commun.*, vol. 61, no. 8, pp. 3156–3169, Aug. 2013.
[36] (2017). *fSONA Corporation*. [Online]. Available: http://www.fsona.com/

AHMED E. MORRA (S'16–M'17) was born in Menoufia, Egypt, in 1984. He received the B.S. and M.S. degrees from the Faculty of Electronic Engineering, Menoufia University, Menouf, Egypt, in 2006 and 2010, respectively, and the Ph.D. degree from the Egypt–Japan University of Science and Technology, Alexandria, Egypt, in 2015, all in electrical engineering.

From 2013 to 2014, he was a Visiting Researcher with the Department of Electrical, Electronics, and Information Engineering, Graduate School of Engineering, Osaka University, Osaka, Japan. In 2015, he joined the Electronics and Electrical Communications Engineering Department, Menoufia University, as an Assistant Professor, where he is currently on leave. From 2015 to 2017, he was an Adjunct Professor with the Center of Photonics and Smart Materials, Zewail City of Science and Technology, Egypt. He is currently a Post-Doctoral Fellow with the Department of Electrical and Computer Engineering, McMaster University, Hamilton, ON, Canada. His research interests are in the areas of free-space and optical wireless communications, optical fiber communications, and photonics engineering.

KHALED AHMED received the B.S. and M.S. degrees from the Faculty of Engineering, Cairo University, Cairo, Egypt, in 2010 and 2015, respectively. He is currently pursuing the Ph.D. degree from McMaster University, Hamilton, ON, Canada.

His current research interests are in the use of free-space optical links in the backhaul of the communication system.

STEVE HRANILOVIC (S'94–M'03–SM'07) received the B.A.Sc. degree (Hons.) in electrical engineering from the University of Waterloo, Canada, in 1997, and the M.A.Sc. and Ph.D. degrees in electrical engineering from the University of Toronto, Canada, in 1999 and 2003, respectively.

From 2010 to 2011, he spent his research leave as a Senior Member of the Technical Staff with Advanced Technology for Research in Motion, Waterloo. He is currently a Professor with the Department of Electrical and Computer Engineering, McMaster University, Hamilton, ON, Canada. He has authored a book entitled *Wireless Optical Communication Systems* (New York: Springer, 2004). His research interests are in the areas of free-space and optical wireless communications, digital communication algorithms, and electronic and photonic implementation of coding and communication algorithms.

Dr. Hranilovic is a Licensed Professional Engineer in the province of Ontario. He received the Government of Ontario Early Researcher Award in 2006. In 2016, the title of University Scholar was conferred upon him by McMaster University. He currently serves as an Associate Editor of the *Journal of Optical Communications and Networking* and an Editor of the IEEE TRANSACTIONS ON COMMUNICATIONS in the area of optical wireless communications.